Adsorption of Sulfur on Ag/Al_2O_3 and Zn/Al_2O_3 Surfaces: Thermal Desorption, Photoemission, and Molecular Orbital Studies

José A. Rodriguez* and Mark Kuhn

Chemistry Department, Brookhaven National Laboratory, Upton, New York 11973

Received: December 9, 1996[⊗]

The interaction of S_2 with Ag/Al_2O_3 and Zn/Al_2O_3 surfaces has been investigated using thermal desorption mass spectroscopy, core- and valence-level photoemission, and ab initio self-consistent-field calculations. The sticking coefficient of S_2 on clean alumina is small (<0.1) at temperatures between 300 and 700 K. In the S_2/Al_2O_3 system, there is an energy mismatch between the orbitals of the molecule and the bands of the oxide, and the reactivity of S_2 on pure alumina is very low. The adsorption of sulfur on Ag/Al_2O_3 and Zn/Al_2O_3 surfaces induces strong perturbations in the electronic properties of the admetals and oxide support. In the Ag/Al_2O_3 and Zn/Al_2O_3 systems, the supported metal clusters (or particles) provide a large number of electronic states that are very efficient at donating charge into the $S_2(2\pi_g)$ orbitals, inducing in this way the breaking of the S−S bond and the formation of admetal sulfides (AgS_x and ZnS_y). The larger the electron transfer from the supported metal into the $S_2(2\pi_g)$ orbitals, the bigger the adsorption energy of the molecule and the easier the cleavage of the S−S bond. The AgS_x and ZnS_y species decompose at temperatures between 750 and 900 K following two different reaction pathways: $AgS_{x,solid} \rightarrow S_{2,gas} + Ag_{solid}$ and $ZnS_{y,solid} \rightarrow S_{2,gas} + Zn_{gas}$.

I. Introduction

One of the best known problems associated with the use of heterogeneous catalysts is the fact that they can be inactivated or poisoned by small amounts of certain substances.[1−3] Probably the most severe poisoning encountered in catalytic systems is that induced by sulfur on supported metal catalysts.[3b] Sulfur-containing molecules are common impurities in crude oil and oil-derived feedstreams.[4] In industrial applications the lifetime of a supported metal catalyst may be reduced to only a few months or weeks in the presence of only ppm quantities of sulfur contaminants in the feed.[3b] At the present time, the intrinsic rates and mechanisms of sulfur poisoning are not fully understood.[3] A fundamental knowledge of the factors that control the interaction of sulfur with metal/oxide interfaces can provide novel ideas for enhancing the sulfur tolerance of industrial catalysts. This work is part of a research program aimed at gaining a better understanding of the effects of sulfur on the physical and chemical properties of metal/oxide surfaces.[5]

Part of the problem in explaining the mechanisms by which sulfur deactivates industrial catalysts arises from the fact that these systems are complex and very difficult to characterize.[3] Model systems generated by vapor-depositing a metal onto ultrathin oxide films have recently emerged as a promising way to investigate the behavior of supported metal catalysts.[6−12] These model systems feature many of the advantages of metal single crystals (i.e., they can be characterized by means of surface sensitive techniques where either electrons or ions are used) while still addressing important issues such as the effects of particle size and metal−support interactions.[7] It has been shown that ultrathin (5−20 Å) films of Al_2O_3 can be grown on a Mo(110) substrate.[7a,7d,13] In a previous work, we used these films to investigate the interaction of Ag and Zn with alumina.[12a] In this article, we examine the adsorption of sulfur on the Ag/Al_2O_3 and Zn/Al_2O_3 surfaces. We deal with admetals that yield sulfides with a large range of heats of formation.[14] Sulfur forms very stable compounds with zinc (ZnS, $\Delta H_f = -46$ kcal/mol[14]). On the other hand, compounds that contain sulfur and silver exhibit a low thermochemical stability (Ag_2S, $\Delta H_f = -8$ kcal/mol[14]).

Previous studies show an identical adsorption/desorption behavior for silver on Al_2O_3 films and on an α-$Al_2O_3(11\bar{2}0)$ single crystal, indicating that the films are a viable model for an α-alumina support.[12b] The films, however, may not be a good model for alumina surfaces that are rich in defect sites and are used as catalyst supports in some industrial processes.[1,2] Silver and zinc do not wet surfaces of alumina well and form three-dimensional (3D) clusters or particles.[12,15] In these systems, the activation energies for desorption of the admetal increase with cluster size (20 kcal/mol for Ag, 10 kcal/mol for Zn).[12] At 300 K the sticking coefficient of Zn on alumina is negligible, whereas that of Ag is close to 0.85 . The deposition of Ag and Zn induces only minor perturbations in the electronic properties of alumina.[12a] Small silver clusters supported on alumina exhibit a partially developed metallic band structure.[12a]

II. Experimental and Theoretical Methods

II.1. Instrumentation. The experiments were performed in an ultrahigh vacuum chamber (base pressure $\leq 3 \times 10^{-10}$ Torr) equipped with a Mg Kα X-ray source, a hemispherical electron energy analyzer with multichannel detection, and a quadrupole mass spectrometer. The mass spectrometer was housed in a differentially pumped liquid nitrogen cooled jacket that has a small aperture in the front. In this arrangement, the mass spectrometer detected only species that desorbed from the "front" face of the sample during thermal desorption experiments.

The total experimental resolution for the photoemission studies was approximately 0.8 eV. In order to enhance surface sensitivity, the sample was positioned such that the takeoff angle for electron detection was 30° off normal. The binding energy scale in the photoemission spectra was calibrated by setting the Zn $2p_{1/2}$ and Ag $3d_{5/2}$ levels of the pure admetals to binding energies of 1044.9 and 368.0 eV, respectively.[16]

* To whom correspondence should be addressed.

[⊗] Abstract published in *Advance ACS Abstracts,* March 15, 1997.

S1089-5647(96)04022-9 CCC: $14.00

The Mo(110) substrate, on which the alumina films were grown, was cleaned following standard procedures reported in the literature.[17] The Mo crystal was mounted on a manipulator capable of liquid nitrogen cooling to 80 K and resistive heating to 1550 K. Heating to 2500 K was achieved by electron bombardment from behind the sample. A W−5% Re/W−26% Re thermocouple was spot-welded to the edge of the Mo(110) sample for temperature measurements.

II.2. Preparation of the Ag/Al_2O_3 and Zn/Al_2O_3 Surfaces. Ultrathin (∼20 Å) films of Al_2O_3 were grown on Mo(110) following a methodology described in previous works.[7d,12a,13] Aluminum atoms (generated by heating a W filament wrapped with a high-purity wire of Al) were dosed to the molybdenum substrate at 700−800 K in a background O_2 pressure of 10^{-5}−10^{-6} Torr, with subsequent annealing to 1200 K to improve the crystalline quality of the alumina films. Silver and zinc were vapor deposited on the Al_2O_3/Mo(110) systems at 300 and 100 K, respectively. The evaporation of Ag (or Zn) was achieved by resistively heating a W filament wrapped by an ultrapure wire of Ag (or Zn). The atomic flux from the metal dosers was calibrated according to the methodology described in our previous studies for Ag/Mo(110)[17a] and Zn/Mo(110).[18] In this work, the amount of Ag or Zn dosed is reported with respect to the number of Mo(110) surface atoms. One equivalent monolayer (ML) of the admetal corresponds to the deposition of 1.43×10^{15} atoms cm^{-2} of Ag or Zn.

The Ag/Al_2O_3 and Zn/Al_2O_3 surfaces were exposed to S_2 gas generated in situ by decomposing Ag_2S in a solid-state electrochemical cell: Pt/Ag/AgI/Ag_2S/Pt.[19] For small doses of gaseous sulfur, the coverage of sulfur on the sample was determined by measuring the area under the S 2p peaks, which was scaled to absolute units by comparing to the corresponding area for 0.9 ML of S on Mo(110).[17,18]

II.3. Molecular Orbital Calculations. The interactions between S_2 and a series of clusters ($ZnAl_4O_6$, $AgAl_4O_6$, Ag_9, and Ag_{10}) were investigated at the ab initio self-consistent-field (SCF) level. The molecular orbital (MO) calculations were performed using the HONDO program.[20] Since the systems under consideration contain a large number of heavy atoms, sulfur was the only element for which we included all its electrons in the calculations. The nonempirical effective core potentials (ECP's) of Wadt and Hay[21] were used to describe the inner shells of Al, Zn, and Ag. The 1s shell of O was described through the ECP generated by Stevens, Basch, and Krauss.[22] The molecular orbitals were expanded using Gaussian-type orbitals (GTO's). The atomic orbitals of S were expressed in terms of a double-zeta quality basis set augmented with polarization functions:[20] twelve s, eight p, and one d primitive GTO's contracted to six s, four p, and one d (12s8p1d/6s4p1d). A basis set obtained through a (3s3p5d/2s1p2d) contraction scheme[23] was used to describe the 4s, 4p, and 3d atomic orbitals of Zn. The 5s, 5p, and 4d atomic orbitals of Ag were expressed in terms of a (3s3p4d/2s1p2d) basis set.[24] Finally, the valence orbitals of O and Al were treated using the basis sets recommended by Stevens−Basch−Krauss[22] and Wadt−Hay,[21b] respectively.

To estimate the charges and orbital populations of the atoms in the clusters, we used a Mulliken population analysis.[25] Due to the limitations of this type of analysis,[26] the charges must not be interpreted in quantitative terms, and we will focus our attention only on qualitative trends. For each cluster, we examined the properties of several possible electronic states with different orbital occupancies and spin multiplicities. The properties reported in section III.4 correspond to those observed for the ground state of each cluster.

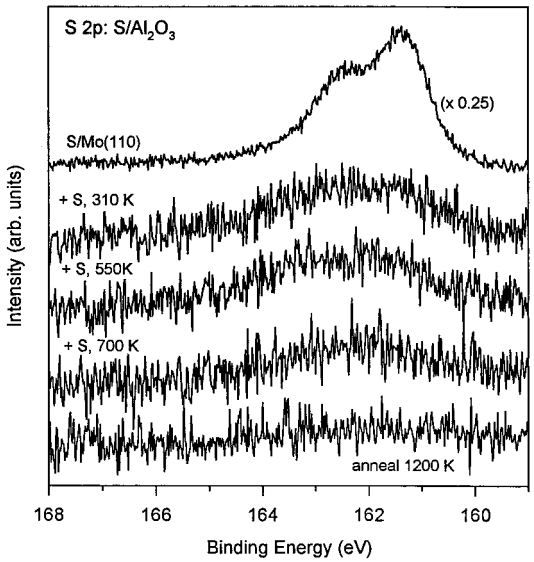

Figure 1. S 2p spectra acquired after dosing S_2 gas to an ultrathin (∼20 Å) film of Al_2O_3 at 310, 550, or 700 K. Before dosing S_2 at 550, or 700 K, the system was annealed to 1200 K to induce the desorption of the sulfur adsorbed in the previous dose. For comparison we also include the S 2p spectrum for 0.9 ML of S on Mo(110).

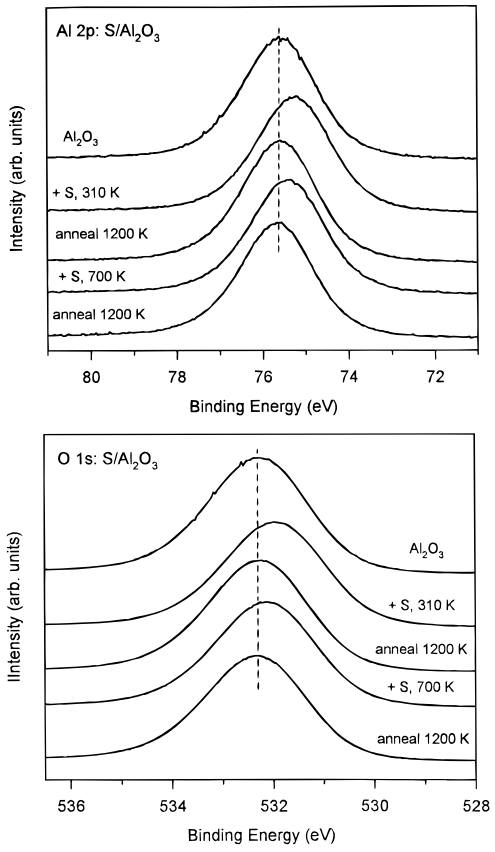

Figure 2. Al 2p (top) and O 1s (bottom) spectra taken after exposing an alumina film to S_2 at 310 or 700 K with subsequent annealing to 1200 K.

III. Results and Discussion

III.1. Reaction of S_2 with Alumina. Figures 1 and 2 display S 2p, Al 2p, and O 1s spectra acquired after dosing S_2 to an ultrathin (∼20 Å) alumina film at 310, 550, or 700 K with subsequent annealing to 1200 K. In these experiments the dose of S_2 was 3−5 times larger than those necessary to saturate a Mo(110) surface with chemisorbed sulfur (θ_S ∼0.9 ML[17]) or to produce sulfide multilayers on metals like Ag,[17a] Zn,[18] and

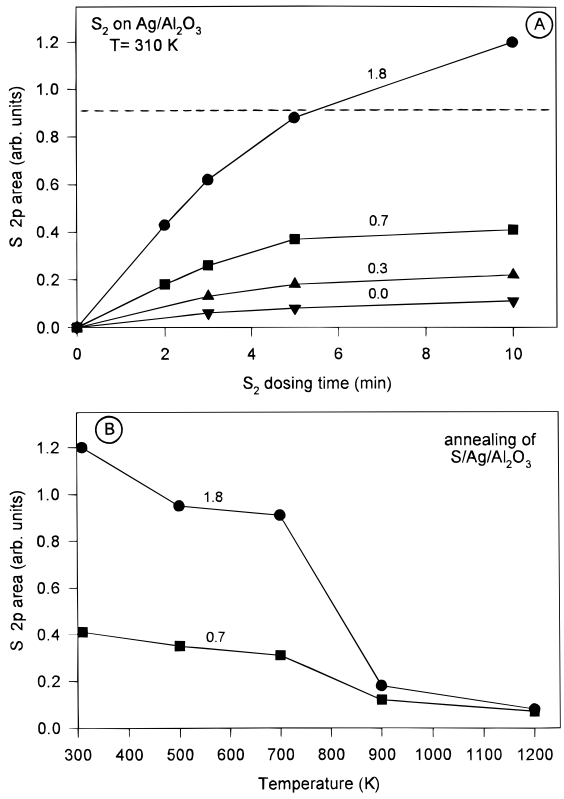

Figure 3. (A) Variation of the S(2p)-integrated signal with S_2 exposure for $S/Ag/Al_2O_3$ surfaces. S_2 was dosed at 310 K. The silver coverages are 0.0, 0.3, 0.7, and 1.8 ML. The dashed line denotes the S 2p area measured for 0.91 ML of S on Mo(110). (B) Effect of annealing temperature on the S(2p)-integrated signal of $S/Ag/Al_2O_3$ surfaces (θ_{Ag} = 0.7 or 1.8 ML).

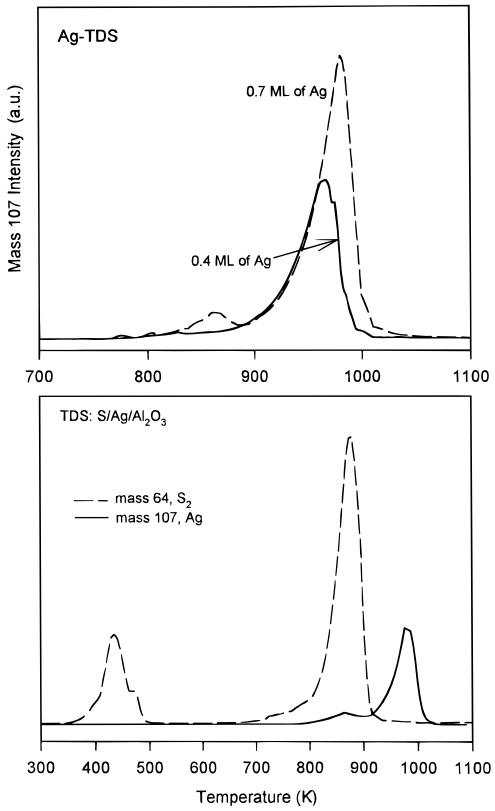

Figure 4. (bottom) S_2 and Ag TDS spectra acquired after depositing ~1.3 ML of sulfur on a Ag/Al_2O_3 surface (θ_{Ag} = 1.7 ML) at 300 K. (top) Ag TDS spectra taken after dosing 5 min of S_2 to Ag/Al_2O_3 surfaces with silver coverages of 0.4 and 0.7 ML at 300 K. No desorption of silver was observed between 300 and 700 K. Heating rate = 5 K/s.

Al.[5a,27] However, on the alumina surface the amount of sulfur adsorbed was very small (≤0.1 ML, Figure 1). These experiments indicate that, overall, the sticking coefficient of S_2 on alumina at 300−700 K is extremely low (<0.1). In Figure 1 the amount of adsorbed sulfur decreases when the temperature of the surface increases: from ~0.1 ML at 310 K to ~0.05 ML at 700 K. Although only a very small fraction of the S_2 molecules that hit the oxide surface dissociated, the chemisorbed sulfur atoms were strongly bound to alumina and were completely removed from the surface only after heating to temperatures around 1200 K. This type of behavior suggests that the S_2 molecules probably dissociated on defect sites that were present on the surface of the alumina film.

One can observe in Figure 2 that the deposition of small amounts of sulfur (0.05−0.10 ML) induces substantial negative shifts (0.4−0.5 eV) in the binding energies of the Al 2p and O 1s features of alumina. An identical behavior was seen for the O *KVV* Auger transition of the oxide (not shown). These binding energy shifts disappear after annealing the S/Al_2O_3 systems to 1200 K and induce the desorption of sulfur. The binding energy shifts may be a consequence of changes in the Fermi level within the band gap of the system due to a transfer of electrons from alumina into sulfur (an electronegative element[28]). Similar binding energy shifts are observed when doping semiconductors and switching from n-type to p-type materials.[8,29] To induce this transformation, only small concentrations of the doping agent are necessary.[29] In a previous study,[12a] we found that small amounts of cesium (an electropositive element[28]) produced a large increase (0.9−1.1 eV) in the binding energy of the core levels and Auger features of alumina. The electronic perturbations observed in the S/Al_2O_3 and Cs/Al_2O_3 surfaces contrast with the behavior found for Ag/Al_2O_3 and Zn/Al_2O_3 surfaces, where submonolayer coverages of Ag and Zn do not induce significant changes in the electronic properties of the oxide.[12a]

III.2. Reaction of S_2 with Ag/Al_2O_3 Surfaces. Figure 3A compares S_2 uptakes on clean Al_2O_3 and Ag/Al_2O_3 surfaces at 310 K. The Ag/Al_2O_3 systems exhibit a much larger reactivity toward S_2 than pure alumina. The total amount of adsorbed sulfur depends strongly on the coverage of silver on the oxide. The dissociation rate of S_2 on the Ag/Al_2O_3 systems was relatively fast until the S/Ag atomic ratio on the surface approached a value of 0.4 . $S/Ag/Al_2O_3$ systems with a S/Ag atomic ratio above 0.8 were not seen in our studies.

Figure 3B illustrates how heating to high temperature affects the S 2p signal of $S/Ag/Al_2O_3$ surfaces. The drops in the S 2p intensity between 300 and 500 K, and 700 and 900 K are accompanied by desorption of S_2. (For a typical result, see bottom of Figure 4). Most of the sulfur remains on/in the sample up to ~700 K. Around 900 K, the amount of sulfur that is left in the system is relatively small (≤0.2 ML). After additional heating to 1200 K the sulfur coverage is reduced to ~0.1 ML. This sulfur was removed by annealing to 1400 K, but the heating also induced decomposition of part of the Al_2O_3 substrate.

Figure 4 shows Ag thermal desorption spectra (mass 107) for $S/Ag/Al_2O_3$ surfaces with 1.7 (bottom), 0.7, and 0.4 ML (top) of silver. Results of photoemission indicated that no Ag remained on the surface after heating to 1100 K. In a previous work we found that Ag desorbs from clean alumina at temperatures between 800 and 1000 K: the larger the size of the Ag clusters (or particles), the higher the desorption temperature.[12a] In Figure 4 most of the Ag desorbs at

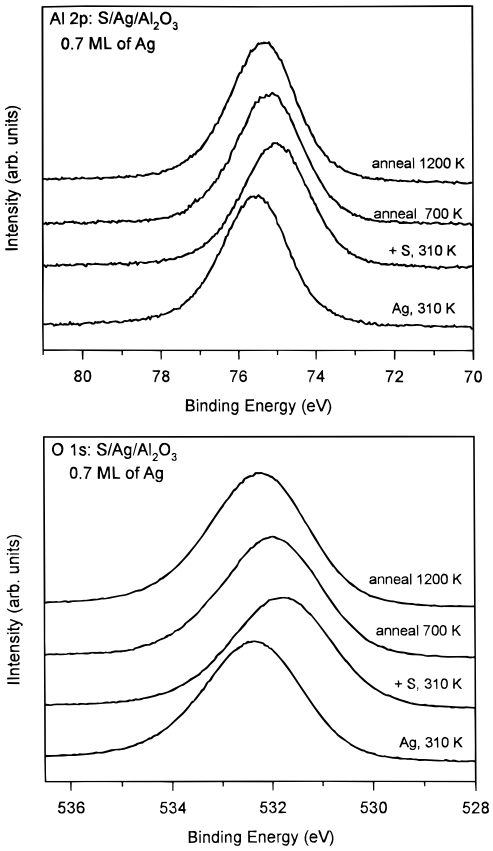

Figure 5. Al 2p (top) and O 1s (bottom) spectra for Ag/Al_2O_3 and $S/Ag/Al_2O_3$ surfaces ($\theta_S = 0.42$ ML, $\theta_{Ag} = 0.70$ ML). Silver and sulfur were dosed at 310 K. The sample was then annealed to 700 and 1200 K.

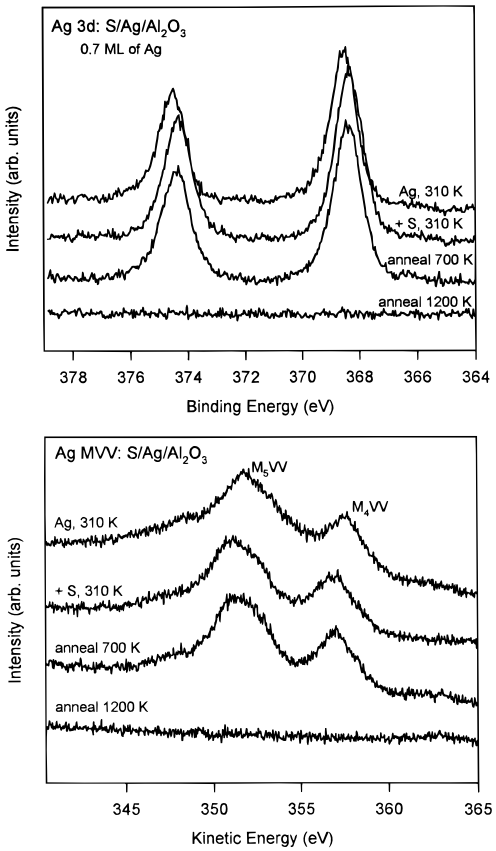

Figure 6. Ag 3d XPS and *MVV* Auger spectra acquired in the same set of experiments that produced the data in Figure 5.

temperatures that are similar to those seen for the desorption of the metal from Ag/Al_2O_3 surfaces. The small Ag desorption feature at ~860 K matches the desorption of S_2 and can be attributed to the desorption of AgS_x species. From the results in Figures 3B and 4 we can conclude that during the heating of a $S/Ag/Al_2O_3$ surface the majority of the sulfur desorbs before the silver at temperatures below 900 K. Then, silver desorbs, and at 1050 K only a small coverage of strongly bound sulfur is left on the oxide.

The trends seen in Figure 3A for the uptake of S_2 indicate that in $S/Ag/Al_2O_3$ systems most of the sulfur is bonded to silver. Evidence for bonding between sulfur and the oxide is provided by the Al 2p and O 1s spectra in Figure 5. After depositing 0.7 ML of Ag on the Al_2O_3 substrate at 310 K, there was no significant change in the binding energy of the Al 2p and O 1s peaks. On the other hand, the adsorption of 0.42 ML of sulfur led to a decrease of 0.6−0.7 eV in the Al 2p and O 1s binding energies. A similar phenomenon was seen after depositing sulfur on clean Al_2O_3 (see Figure 2). In Figure 5, one can see an increase in the binding energy of the Al 2p and O 1s levels of the $S/Ag/Al_2O_3$ surface upon heating to 700 and 1200 K, which is probably a consequence of the desorption of sulfur.

The photoemission results in Figures 6 and 7 illustrate the effects of sulfur on the 3d core levels, *MVV* Auger transitions, and 4d valence band of silver clusters supported on alumina. The adsorption of sulfur induced a reduction of ~0.3 eV in the Ag 3d peak positions (top of Figure 6). These binding energy shifts can be attributed to the formation of AgS_x species on the oxide, since a $4Ag_{solid} + S_{2,gas} \rightarrow 2Ag_2S_{solid}$ transformation leads to a negative shift of ~0.15 eV in the binding energy of the Ag 3d peaks.[30,31] The Ag M_5VV and M_4VV Auger transitions of the Ag/Al_2O_3 systems showed large positive binding energy shifts (0.6−0.8 eV) upon the adsorption of sulfur (bottom of Figure 6). This behavior also indicates the formation of AgS_x compounds.[30,31] After heating the $S/Ag/Al_2O_3$ surfaces to high temperature, the Ag photoemission features associated with AgS_x species were seen up to around 750 K. At this temperature the decomposition of the silver sulfides probably started: $AgS_{x,solid} \rightarrow S_{2,gas} + Ag_{solid}$.

Figure 7 displays valence spectra taken after dosing S_2 to a thick polycrystalline Ag film (top panel) and a Ag/Al_2O_3 surface (bottom panel). Since the valence region was examined using Mg Kα radiation, the intensity of electron emissions from the sulfur levels and alumina bands is very weak, and the valence spectra are dominated by electron emissions from the Ag 4d band. Ag clusters supported on alumina exhibit a 4d band somewhat narrower than that of pure metallic Ag.[12a] In Figure 7 there is a large decrease in the width of the Ag 4d band upon the adsorption of sulfur on Ag and Ag/Al_2O_3. This narrowing of the Ag 4d band is a consequence of a large reduction in the strength of the Ag(4d) ↔ Ag(4d) interactions,[32] and suggests that the interactions between the Ag(4d) and S(3s,3p) orbitals are weak. The molecular orbital studies discussed in section III.4 show a lack of active participation of the Ag(4d) orbitals in the Ag−S bond.

In summary, the results discussed in this section for the $S/Ag/Al_2O_3$ surfaces show that sulfur induces strong perturbations in the electronic properties of silver and alumina. Silver clusters supported on alumina react with sulfur, forming AgS_x compounds that decompose at temperatures between 750 and 900 K. These temperatures are much bigger than those typically used in industrial processes that involve Ag/Al_2O_3 catalysts (400−650 K[33]).

III.3. Reaction of S_2 with Zn/Al_2O_3 Surfaces. Figure 8 shows how the amount of sulfur adsorbed on Zn/Al_2O_3 surfaces at 300 K varies with S_2 exposure and zinc coverage. The Zn/

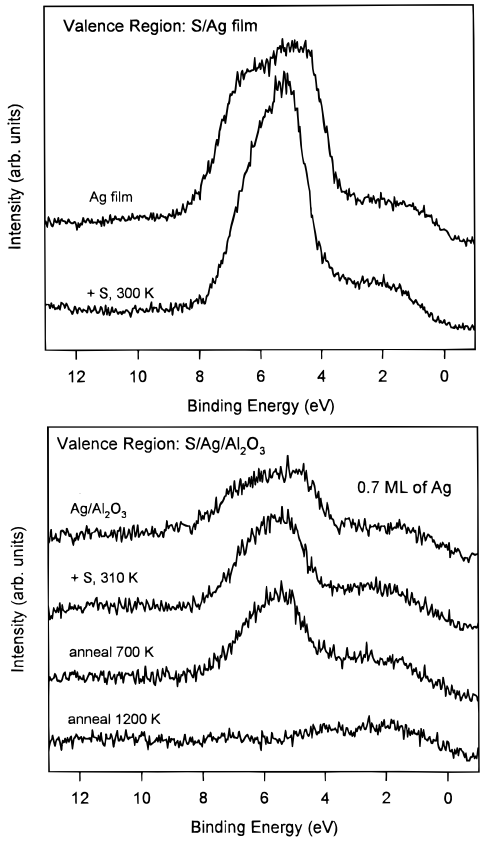

Figure 7. (top) Valence spectra taken before and after dosing S_2 to a thick polycrystalline Ag film. (bottom) Valence spectra acquired before and after depositing 0.42 ML of sulfur on a Ag/Al_2O_3 surface (θ_{Ag} = 0.70 ML). The sulfur was dosed at 310 K, and this was followed by annealing of the sample to 700 and 1200 K. The electrons were excited using Mg Kα radiation.

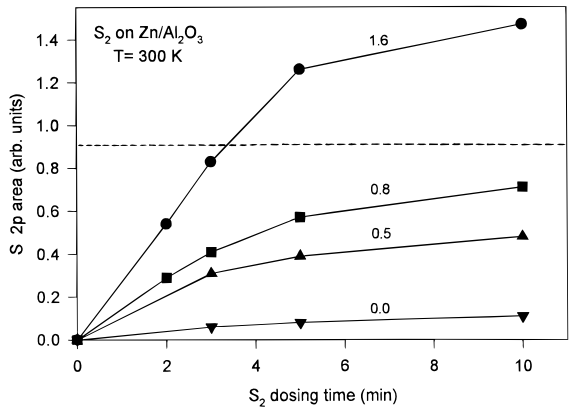

Figure 8. Variation of S(2p)-integrated signal with S_2 exposure for $S/Zn/Al_2O_3$ surfaces (θ_{Zn} = 0.0, 0.5, 0.8, and 1.6). The dashed line denotes the S 2p area measured for 0.91 ML of S on Mo(110). Zinc was vapor deposited on alumina at 100 K. Then, the Zn/Al_2O_3 surfaces were exposed to S_2 gas at 300 K.

Al_2O_3 surfaces display a much larger reactivity toward S_2 than clean alumina. As in the case of the Ag/Al_2O_3 systems, the total amount of sulfur adsorbed on a Zn/Al_2O_3 surface increases when the coverage of the admetal is raised. After comparing the results in Figures 3A and 8, one can conclude that on a per-admetal atom basis the uptake of sulfur by a Zn/Al_2O_3 surface is larger than that by a Ag/Al_2O_3 surface. In Figure 3A the S/Ag atomic ratio is never larger than 0.7, whereas in Figure 8 the S/Zn atomic ratio reaches values around 0.9 . This difference may be due to the fact that compounds with a S/Zn ratio close to 1:1 are thermodynamically more stable than

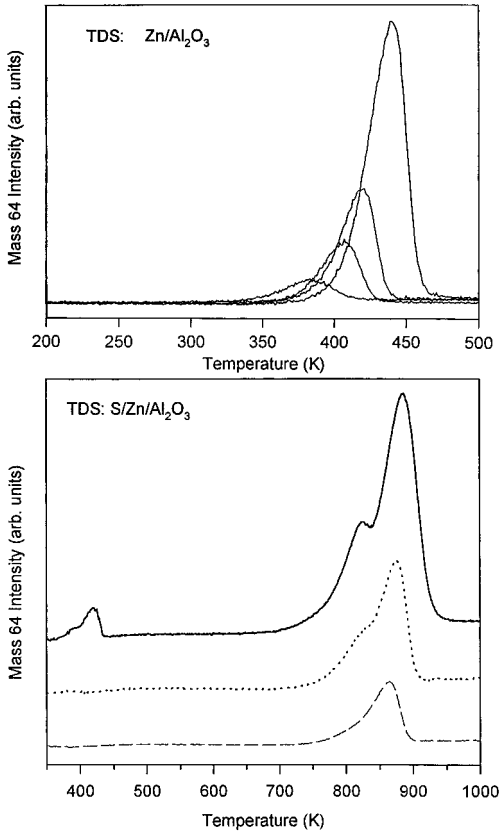

Figure 9. (top) Zinc thermal desorption spectra (mass 64) for a series of Zn/Al_2O_3 surfaces (θ_{Zn} = 0.3, 0.8, 1.7, and 4.2 ML). (bottom) Mass 64 thermal desorption spectra (Zn and S_2) for $S/Zn/Al_2O_3$ surfaces. Zinc was vapor deposited on alumina at 100 K (θ_{Zn} = 0.3, 0.7, and 1.8 ML). Then, the Zn/Al_2O_3 surfaces were exposed to S_2 for 10 min. Heating rate = 5 K/s.

compounds with a similar S/Ag stoichiometry.[14] In addition, the cohesive energy of metallic zinc is smaller than that of metallic silver,[34] making easier the penetration of sulfur into zinc particles.

Thermal desorption spectra for Zn/Al_2O_3 and $S/Zn/Al_2O_3$ surfaces are shown in Figure 9. Zinc desorbs from clean alumina at temperatures between 350 and 480 K. As the size of the supported Zn clusters increases, they become more stable, and there is a shift toward higher temperature in the Zn desorption features.[12a] In the case of $S/Zn/Al_2O_3$ surfaces it is not possible to distinguish between the desorption peaks of Zn and S_2 since both appear at mass 64. However, it is clear that the formation of Zn−S bonds leads to an increase of ∼ 350 K in the thermal stability of zinc on the oxide surface. In the TDS experiments with the $S/Zn/Al_2O_3$ surfaces, no signal was detected for masses 96 (ZnS) and 128 (ZnS_2).

The desorption peaks in the bottom panel of Figure 9 can be assigned with the help of the photoemission data in Figure 10. This figure shows the effects of annealing temperature on the S 2p and Zn $2p_{1/2}$ areas of three different $S/Zn/Al_2O_3$ surfaces. At temperatures between 300 and 700 K there are only minor changes in the S 2p and Zn $2p_{1/2}$ intensities. From 700 to 900 K, one can see a large simultaneous reduction in the signal of both core levels. At 1100 K all the zinc has desorbed from the surface, and only a relatively small amount of sulfur (0.10−0.15 ML) remains on the oxide. Thus, the desorption features between 700 and 900 K in Figure 9 probably come from simultaneous desorption of Zn and S_2. Once the Zn−S bonds are broken at 700−900 K, then zinc and sulfur desorb together since they are not stable on the oxide at these high temperatures.

The deposition of sulfur on the Zn/Al_2O_3 surfaces produced

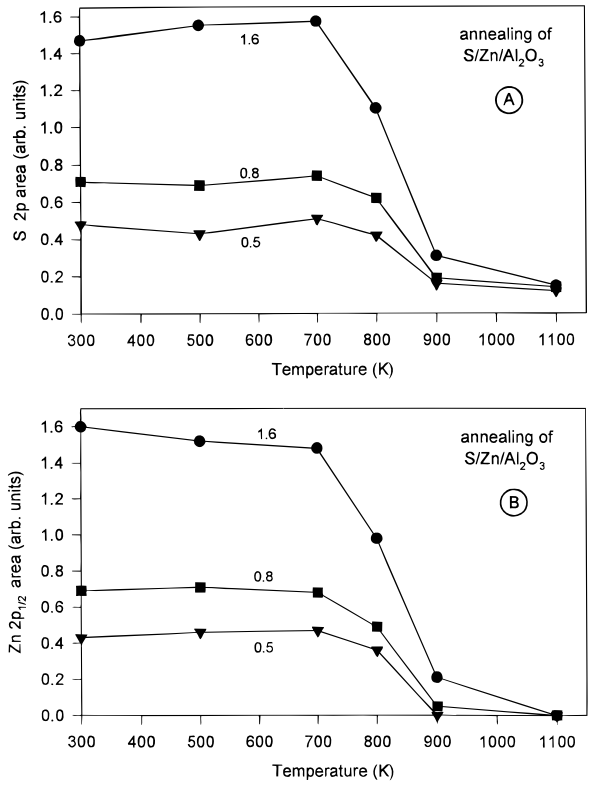

Figure 10. Effect of annealing temperature on the S(2p)- and Zn-($2p_{1/2}$)-integrated signal of $S/Zn/Al_2O_3$ surfaces (θ_{Zn} = 0.5, 0.8, and 1.6).

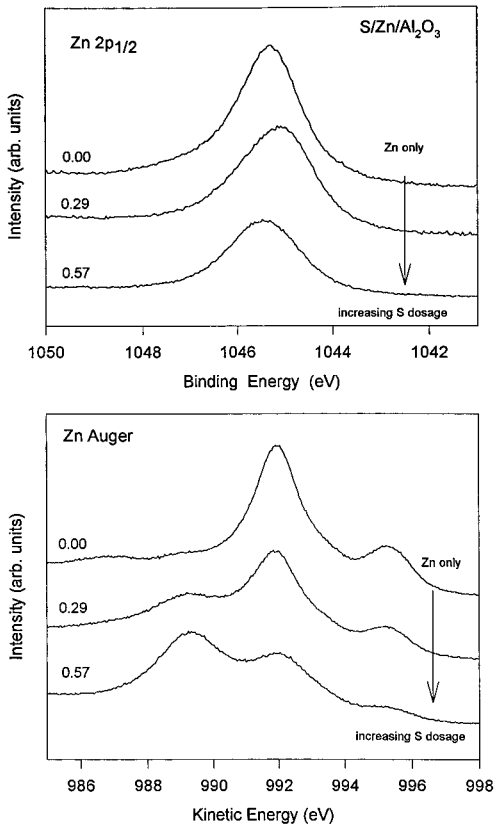

Figure 11. Zn $2p_{1/2}$ (top) and Zn *LMM* Auger spectra (bottom) acquired before and after adsorbing 0.29 and 0.57 ML of sulfur on a Zn/Al_2O_3 surface (θ_{Zn} = 0.8) at 300 K. The primary electrons were excited with Mg Kα radiation.

substantial (0.6−0.8 eV) negative shifts in the binding energy of the Al 2p and O 1s levels, as happened in the S/Al_2O_3 and $S/Ag/Al_2O_3$ systems. Figure 11 shows Zn $2p_{1/2}$ and Zn *LMM* Auger spectra acquired after depositing 0.29 and 0.57 ML of sulfur on a Zn/Al_2O_3 surface (θ_{Zn}= 0.8 ML) at 300 K. In these experiments one can see the progressive transformation of metallic Zn into ZnS_x species. The formation of bulk ZnS from metallic Zn is accompanied by a substantial (∼0.5 eV) positive binding energy shift in the Zn 2p levels and a large (3−3.5 eV) increase in the kinetic energy of the Zn *LMM* Auger transitions.[35] In Figure 11 the Zn Auger features with a kinetic energy of ∼989.5 eV indicate the presence of ZnS_x compounds in the $S/Zn/Al_2O_3$ surface.

In many aspects the behavior seen for the $S/Zn/Al_2O_3$ and $S/Ag/Al_2O_3$ surfaces is very similar. In these systems sulfur modifies the electronic properties of the oxide and forms compounds with the admetal that decompose at temperatures above 700 K. An important difference appears in the reaction pathways for the decomposition of the admetal sulfides. In the case of $S/Ag/Al_2O_3$ systems, the dissociation of the metal sulfide (AgS_x) produces S_2 that goes into gas phase, and the metal remains on the surface. On the other hand, in $S/Zn/Al_2O_3$ systems the metal sulfide is more stable than the pure metal, and when ZnS_x decomposes, the admetal and sulfur desorb simultaneously. In this sense, the $S/Ag/Al_2O_3$ and $S/Zn/Al_2O_3$ systems illustrate two different routes for the decomposition of supported metal sulfides.

III.4. Interaction of S_2 with Zn/Al_2O_3, Ag/Al_2O_3 and Ag-(111) Surfaces. In this section we investigate the bonding of S_2 to Zn/Al_2O_3, Ag/Al_2O_3, and Ag(111) surfaces using ab initio SCF calculations. We will focus our attention only on admetal ↔ sulfur interactions. The photoemission and thermal desorption experiments described above indicate that the reaction of S_2 with Zn/Al_2O_3 and Ag/Al_2O_3 surfaces involves mainly interactions between sulfur and the supported metal particles (or clusters). The oxide support plays only a minor role. There are strong similarities in the behavior seen here for $S/Ag/Al_2O_3$ and that reported for S/Ag(111) systems.[36] On Ag(111) at 300 K, S_2 undergoes dissociative chemisorption that leads to the formation of a Ag_2S film.[36] This film decomposes at temperatures between 650 and 800 K with S_2 evolving into gas phase.[36] Thus, in Ag/Al_2O_3 surfaces the supported metal clusters probably expose faces similar to the close-packed (111) plane of Ag.

Figure 12 shows the clusters on which the S_2 molecule was adsorbed. Cluster I ($ZnAl_4O_6$ or $AgAl_4O_6$) is a model for a metal atom supported on a defect site of alumina in which the oxygens have a relatively low coordination number. On this site, the admetal ↔ oxide interactions are expected to be much stronger than on a perfect flat Al_2O_3 surface. Thus, when examining the adsorption of S_2 on cluster I, one is dealing with a situation in which the oxide support can induce large perturbations in the reactivity of the admetal toward sulfur. On the other hand, the adsorption of S_2 on clusters II (Ag_{10}) and III (Ag_9) represents the case in which the oxide support does not affect the chemistry of S_2 on the admetal. Cluster III also provides a model for studying the interaction of S_2 with a Ag-(111) surface or Ag(111)-like particles.

In cluster I, the Al−O bond distances were all set equal to 1.91 Å (an average of the distances found in alumina[37]), the O−Al−O bond angles were 90°, and the admetal−O_2 distances were optimized at the ab initio SCF level obtaining values of 2.03 (Zn−O_2) and 2.11 Å (Ag−O_2). These values are close to bond lengths seen in compounds that contain oxygen and zinc[38] or oxygen and silver.[39] In clusters II and III, the Ag−Ag bond lengths and angles were set equal to those observed in bulk silver.[40] Figure 13 displays the bonding configurations of S_2 when the molecule was adsorbed on a-top sites of clusters I, II,

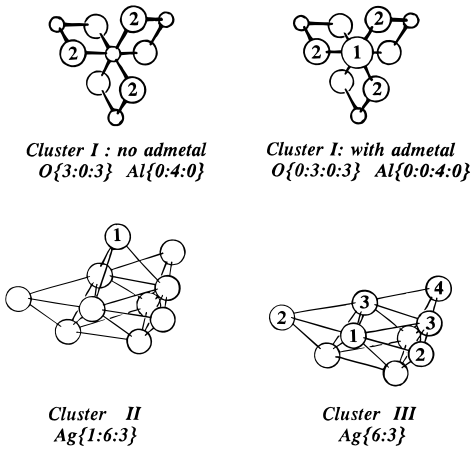

Figure 12. Clusters used to model Zn/Al_2O_3, Ag/Al_2O_3, and Ag(111) surfaces. In cluster I ($ZnAl_4O_6$ or $AgAl_4O_6$), the admetal sits on the center of the 3-fold hollow formed by the oxygens labeled "2". Cluster I has four layers, with the admetal atom in the first layer, three O atoms in the second, four Al atoms in the third, and three O atoms in the fourth. Cluster II (Ag_{10}) and III (Ag_9) have three and two layers, respectively. In these clusters the Ag atoms are arranged in the geometry expected for bulk silver. In cluster II, the admetal atom labeled "1" sits on a 3-fold hollow site of a (111) plane of Ag atoms.

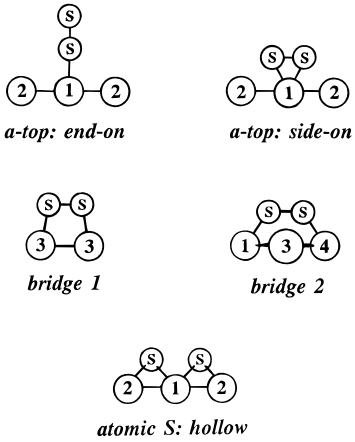

Figure 13. Geometries investigated for the adsorption of S_2 on cluster III. The S_2 molecule was adsorbed on top of the Ag atom labeled "1" (end-on or side-on configurations), on the short bridge site formed by the atoms labeled "3", and on the long bridge (or pseudohollow) site formed by the atoms labeled "1" and "4". Two sulfur atoms were adsorbed on the 3-fold hollow sites generated by the atoms labeled "1", "2", and "3". We also studied the adsorption of S_2 on clusters I and II, with the molecule adsorbed on top of the metal atom labeled "1" in end-on or side-on configurations.

and III or on bridges sites of cluster III. Table 1 lists the optimal values found in our calculations for the Zn−S, Ag−S, and S−S bond lengths in the adsorption models. For the free S_2 molecule, the calculated S−S bond distance (1.88 Å) agrees very well with the reported experimental value (1.89 Å[41]). The adsorption of the molecule produces a significant increase (0.06−0.25 Å) in the S−S separation. The values predicted by our SCF calculations for the Zn−S (2.32−2.39 Å) and Ag−S (2.48−2.62 Å) bond lengths are similar to those observed in X-ray diffraction studies for inorganic complexes that contain Zn−S or Ag−S bonds.[42]

Figure 14 shows the energies calculated in this work for the valence "bands" of the Al_4O_6 and Ag_{10} clusters. The results for bulk alumina come from band-structure calculations,[43] whereas the position for the valence bands of bulk silver was estimated using work function measurements[44] and photoemission data.[45] In bulk alumina the O 2p band is fully occupied, the Al 3s,p band is empty, and there are unoccupied surface

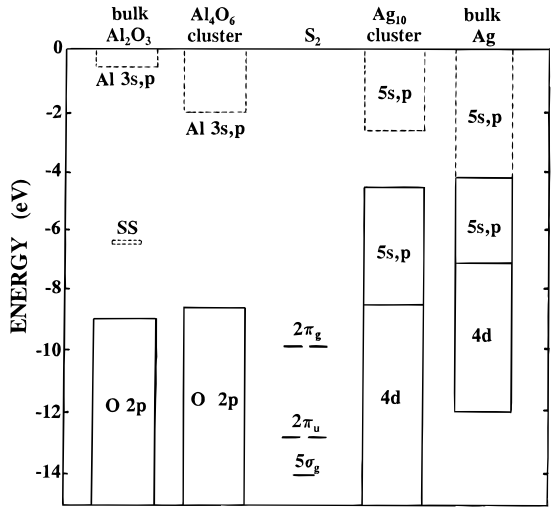

Figure 14. Energy positions for the bands of bulk alumina,[43] bulk silver,[44,45] and the Al_4O_6 and Ag_{10} clusters. The empty and occupied states are indicated by dashed and solid lines, respectively. The label "SS" refers to surface states in alumina.[43] For comparison, we also include the calculated energies for the $5\sigma_g$, $2\pi_u$, and $2\pi_g$ orbitals of the S_2 molecule. The energies are reported with respect to the vacuum level.

TABLE 1: Adsorption of S_2 on Zn/Al_2O_3, Ag/Al_2O_3, and Ag(111)

configuration	metal−S bond (Å)	S−S bond (Å)	charge on S_2 (*e*)	adsorption energy (kcal/mol)
free S_2		1.88	0.00	
S_2 on $ZnAl_4O_6$				
end-on	2.32	1.94	−0.04	8
side-on	2.39	1.96	−0.06	5
S_2 on $AgAl_4O_6$				
end-on	2.56	1.96	−0.04	9
side-on	2.63	1.99	−0.08	7
S_2 on Ag_{10}				
end-on	2.51	2.03	−0.14	14
side-on	2.62	2.06	−0.18	13
S_2 on Ag_9				
end-on	2.48	1.99	−0.11	10
side-on	2.60	2.02	−0.13	12
bridge 1	2.56	2.09	−0.18	17
bridge 2	2.61	2.13	−0.24	22
atomic S (hollow)	2.52	2.88	−0.78	36

states ("SS" in Figure 14) within the band gap.[43,46] The band gap observed in the SCF calculations for the Al_4O_6 cluster is close to that seen in bulk alumina. The band structure predicted by the SCF calculations for the Ag_{10} cluster is in general agreement with that observed for bulk silver, but in the theoretical results the Ag 4d orbitals appear at higher binding energy than in photoemission measurements. This is because the SCF Koopmans' theorem ionization potentials given by the MO energies of the Ag_{10} cluster do not include final-state relaxation, which is expected to be considerably large for valence d orbitals.[47]

In Figure 14 we also include the calculated energies for the highest occupied MO's of free (gas phase) S_2, which are in good agreement with the corresponding ionization potentials.[41,48] The ground $^3\Sigma^-_g$ state of the molecule arises from a $4\sigma_g^2 4\sigma_u^2 5\sigma_g^2 2\pi_u^4 2\pi_g^2$ electronic configuration. The $2\pi_g$ orbitals are only half-occupied and are S−S antibonding. In principle, the bonding mechanism of S_2 to an oxide or metal can involve donation of charge from the $2\pi_u$ and $5\sigma_g$ orbitals of the molecule into the surface and back-donation of electrons from the surface into the $S_2(2\pi_g)$ orbitals. An analysis of the results in Figure 14 shows that the occupied states of S_2 are well separated from the empty bands of alumina and silver, making difficult sulfur

→ substrate electron-donor interactions. In the case of S_2/Al_2O_3, the lowest unoccupied orbitals of the molecule ($2\pi_g$'s) are not much more stable than occupied states in the valence O 2p band of the oxide. This leads to relatively weak $Al_2O_3 \rightarrow S_2(2\pi_g)$ electron-donor interactions, and therefore the sticking coefficient and reactivity of S_2 on surfaces of pure alumina are low. For Ag/Al_2O_3 and Zn/Al_2O_3 surfaces, the supported metal clusters (or particles) provide a large number of states that are very efficient at donating electrons to the $S_2(2\pi_g)$ orbitals, inducing in this way the breaking of the S−S bond and the formation of admetal sulfides.

In Table 1 are listed calculated adsorption energies for S_2 on clusters I, II, and III. For the diatomic AgS molecule our SCF calculations predict a dissociation energy of 31 kcal/mol, which is smaller than the experimental value of 52 kcal/mol.[49] Thus, it is likely that the values listed in Table 1 underestimate the bonding energy of S_2 on the clusters. When dealing with adsorption energies, we will pay more attention to qualitative trends than to quantitative results. On the $ZnAl_4O_6$, $AgAl_4O_6$, and Ag_{10} clusters the S_2 molecule was bonded only to one admetal atom (labeled "1" in Figure 12). In these systems, the charge on the adsorption sites before the adsorption of S_2 was +0.41 *e* in $ZnAl_4O_6$, +0.29 *e* in $AgAl_2O_3$, and +0.07 *e* in Ag_{10}. In the $ZnAl_4O_6$ and $AgAl_4O_6$ clusters, there is a shift of electrons from the admetal toward the oxide support (Al_4O_6 unit) that reduces the reactivity of the admetal toward S_2. When S_2 is bonded to $ZnAl_4O_6$ and $AgAl_4O_6$ clusters, one sees adsorption energies, S_2 charges, and S−S bond distances that are smaller than those seen for the adsorption of the molecule on pure metal clusters (Ag_{10} and Ag_9). The reader should keep in mind that cluster I represents a metal atom sitting on a defect site of alumina and, therefore, it maximizes the effects of the oxide support on the reactivity of the admetal. The results for the bonding of S_2 to clusters II and III probably provide a better representation for the most relevant phenomena that occur during the adsorption of S_2 on Ag/Al_2O_3 surfaces.

On cluster III, Ag(111)-like surface, the S_2 molecule is more stable when both S atoms are simultaneously bonded to the metal substrate. This is reminiscent of the behavior observed for O_2 on silver single crystals, where the molecule chemisorbs with its O−O axis parallel to the surface.[50] For the adsorption of S_2 on cluster III, the larger the charge transfer from Ag into the $S_2(2\pi_g)$ orbitals, the bigger the adsorption energy and the elongation of the S−S bond. Bonding configurations in which S_2 bridges two silver atoms ("bridge 1" and "bridge 2" in Figure 13) are probable precursors for the dissociation of the molecule. In the SCF calculations we found that two separate sulfur adatoms were much more stable on the surface of cluster III than adsorbed S_2 in end-on, side-on, or bridge conformations. Therefore, S_2 should dissociate when adsorbed on clean silver particles.

After adsorbing a single S atom on cluster III, we found adsorption energies on hollow sites that were 8−11 kcal/mol larger than on a-top sites or 6−8 kcal/mol larger than on bridges sites. Thus, S should sit on hollow sites of Ag(111)-like surfaces at low coverages. Experimental studies have shown that atomic sulfur prefers to adsorb on hollow sites when present on close-packed surfaces of transition metals.[51] Sulfur behaved as an electron acceptor when bonded to cluster III, with the charge on the S atom varying from −0.31 to −0.53 *e*. It is known that sulfur increases the work function of Ag(111),[36] a phenomenon consistent with a Ag → S charge transfer. On average, the charge for S on hollow sites of cluster III was ∼0.15 *e* less negative than on a-top sites. An identical trend was seen in our previous study for S/Pt(111).[52] In these systems, the negative charge on the S atoms is mainly a consequence of a metal → S(3p) electron transfer. For hollow adsorption, the S adatoms are forced to make bonds through their occupied 3s and 3p orbitals. This leads to a more covalent adsorption bond, in which part of the charge that is transferred from the surface into the vacant S(3p) orbitals is compensated by charge transfer from the occupied S(3s,3p) orbitals into the empty bands of the metal substrate.

The photoemission results in Figure 7 show a large decrease in the width of the Ag 4d band after the formation of AgS_x species. This narrowing of the Ag 4d band is a consequence of a large reduction in the strength of the Ag(4d) ↔ Ag(4d) interactions and weak Ag(4d) ↔ S(3s,3p) interactions. For example, SCF calculations for Ag_2 show the 4d orbitals of the molecule spread out in a range of 1.8 eV, whereas the corresponding calculations for AgS show 4d orbitals that appear in a range of only 0.3 eV (quasi-atomic behavior). A lack of active participation of the Ag 4d orbitals in the Ag−S bond is consistent with the results of ab initio SCF calculations for molecules containing silver (AgO,[53] AgH,[53a] AgLi[32]) and INDO-MO calculations for the adsorption of sulfur compounds (SH,[54a] SO_2,[54b] SO_4,[54c] CH_3S[54d]) on silver surfaces. In all these cases, the Ag 4d orbitals are almost not involved in chemical bonding.

IV. Summary and Conclusions

In the S_2/Al_2O_3 system, there is an energy mismatch between the orbitals of the molecule and the bands of the oxide, and the sticking coefficient of S_2 on clean alumina is very small (<0.1) at temperatures between 300 and 700 K. The deposition of sulfur on Al_2O_3 induces strong perturbations in the electronic properties of the oxide. The reactivity of Ag/Al_2O_3 and Zn/Al_2O_3 surfaces toward sulfur is much larger than that of pure Al_2O_3. In the Ag/Al_2O_3 and Zn/Al_2O_3 systems, the supported metal clusters (or particles) provide a large number of electronic states that are very efficient at donating charge to the $S_2(2\pi_g)$ orbitals, inducing in this way the breaking of the S−S bond and the formation of admetal sulfides. For the adsorption of S_2 on Ag(111)-like clusters, the larger the electron transfer from Ag into the $S_2(2\pi_g)$ orbitals, the bigger the adsorption energy and the elongation of the S−S bond. The most stable adsorption geometries of S_2 (probable precursors for the dissociation of the molecule) involve bonding of both S atoms to the metal substrate.

The reaction of S_2 with silver and zinc clusters supported on alumina produces AgS_x ($x < 0.8$) and ZnS_y ($y < 0.95$) compounds that decompose at temperatures between 750 and 900 K. Two different reaction pathways were observed for the decomposition of these sulfides: $AgS_{x,solid} \rightarrow S_{2,gas} + Ag_{solid}$ and $ZnS_{y,solid} \rightarrow S_{2,gas} + Zn_{gas}$.

Acknowledgment. This work was carried out at Brookhaven National Laboratory and supported by the U.S. Department of Energy (DE-AC02-76CH00016), Office of Basic Energy Sciences, Chemical Science Division.

References and Notes

(1) Bond, G. C. *Heterogeneous Catalysis: Principles and Applications*; 2nd ed.; Oxford: New York, 1987.

(2) Gates, B. C. *Catalytic Chemistry*; Wiley: New York, 1992.

(3) (a) Menon, P. G. *Chem. Rev.* **1994**, *94*, 1021. (b) Bartholomew, C. H.; Agrawal, P. K.; Katzer, J. R. *Adv. Catal.* **1982**, *31*, 135. (c) Oudar, J., Wise, H., Eds. *Deactivation and Poisoning of Catalysts*; Marcel Dekker: New York, 1983.

(4) Speight, J. G. *The Chemistry and Technology of Petroleum*, 2nd ed.; Marcel Dekker: New York, 1991.

(5) (a) Rodriguez, J. A.; Kuhn, M.; Hrbek, J. *Surf. Sci.*, in press. (b) Chaturvedi, S.; Rodriguez, J. A.; Hrbek, J. Manuscript in preparation.

(6) Chen, J. G.; Colaianni, M. L.; Weinberg, W. H.; Yates, J. T. *Surf. Sci.* **1992**, *279*, 223 and references therein.
(7) (a) Goodman, D. W. *Chem. Rev.* **1995**, *95*, 523. (b) Xu, X.; Vesecky, S. M.; Goodman, D. W. *Science* **1992**, *258*, 788. (c) Coulter, K.; Xu, X.; Goodman, D. W. *J. Phys. Chem.* **1994**, *98*, 1245. (d) Wu, M.-C.; Oh, W. S.; Goodman, D. W. *Surf. Sci.* **1995**, *330*, 61. (e) Rainer, D. R.; Xu, C.; Holmblad, P. M.; Goodman, D. W. *J. Vac. Sci. Technol. A*, submitted for publication.
(8) Campbell, C. T. *Surf. Sci. Rep.*, in press.
(9) (a) Wu, Y.; Garfunkel, E.; Madey, T. E. *J. Vac. Sci. Technol. A* **1996**, *14*, 1662. (b) Zhou, J. B.; Lu, H. C.; Gustafsson, T.; Garfunkel, E. *Surf. Sci.* **1993**, *293*, L887.
(10) Freund, H.-J.; Kuhlenbeck, H.; Staemmler, V. *Rep. Prog. Phys.* **1996**, *59*, 283.
(11) (a) Altman, E. I.; Gorte, R. J. *Surf. Sci.* **1986**, *172*, 71. (b) Fritsch, A.; Légaré, P. *Surf. Sci.* **1987**, *184*, L355. (c) Venus, D.; Hensley, D. A.; Kesmodel, L. L. *Surf. Sci.* **1988**, *199*, 391. (d) Cordatos, H.; Bunluesin, T.; Stubenrauch, J.; Vohs, J. M.; Gorte, R. J. *J. Phys. Chem.* **1996**, *100*, 785.
(12) (a) Rodriguez, J. A.; Kuhn, M.; Hrbek, J. *J. Phys. Chem.* **1996**, *100*, 18240. (b) Van Campen, D. G.; Hrbek, J. *J. Phys. Chem.* **1995**, *99*, 16389.
(13) Chen, P. J.; Colaianni, M. L.; Yates, J. T. *Phys. Rev. B* **1990**, *15*, 8025.
(14) *Lange's Handbook of Chemistry*, 13th ed.; McGraw-Hill: New York, 1985; pp 9−53, 9−68.
(15) Beitel, G.; Markert, K.; Wiechers, J.; Hrbek, J.; Behm, R. In *Adsorption on Ordered Surfaces of Ionic Solids and Thin Films*; Umbach, E., Freund, H. J., Eds; Springer-Verlag: Berlin, 1993; pp 71−82.
(16) Williams, G. P. *Electron Binding Energies of the Elements*, Version II; National Synchrotron Light Source, Brookhaven National Laboratory: Upton, NY, 1992.
(17) (a) Rodriguez, J. A.; Kuhn, M. *J. Phys. Chem.* **1995**, *99*, 9567. (b) Kuhn, M.; Rodriguez, J. A. *Surf. Sci.* **1996**, *355*, 85.
(18) Kuhn, M.; Rodriguez, J. A. *Surf. Sci.* **1995**, *336*, 1.
(19) (a) Heegeman, W.; Meister, K. H.; Betchold, E.; Hayek, K. *Surf. Sci.* **1975**, *49*, 161. (b) Xu, G.-Q.; Hrbek, J. *Catal. Lett.* **1989**, *2*, 35.
(20) Dupuis, M.; Chin, S.; Marquez, A. In *Relativistic and Electron Correlation Effects in Molecules and Clusters*; Malli, G. L., Ed.; NATO ASI Series; Plenum: New York, 1992.
(21) (a) Hay, P. J.; Wadt, W. R. *J. Chem. Phys.* **1985**, *82*, 270. (b) Wadt, W. R.; Hay, P. J. *J. Chem. Phys.* **1985**, *82*, 284.
(22) Stevens, W. J.; Basch, H.; Krauss, M. *J. Chem. Phys.* **1984**, *81*, 6026.
(23) Rodriguez, J. A.; Kuhn, M. *J. Phys. Chem.* **1996**, *100*, 381.
(24) Rodriguez, J. A.; Kuhn, M. *J. Phys. Chem.* **1994**, *98*, 11251.
(25) Mulliken, R. S. *J. Chem. Phys.* **1955**, *23*, 1841.
(26) Szabo, A.; Ostlund, N. S. *Modern Quantum Chemistry*; McGraw-Hill: New York, 1989.
(27) Kuhn, M.; Rodriguez, J. A.; Hrbek, J. *Surf. Sci.* **1996**, *365*, 53.
(28) Moeller, T. *Inorganic Chemistry*; Wiley: New York, 1982; pp 82−83.
(29) Egelhoff, W. F. *Surf. Sci. Rep.* **1987**, *6*, 253.
(30) Kaushik, V. K. *J. Electron Spectrosc. Relat. Phenom.* **1991**, *56*, 273.
(31) Kuhn, M.; Rodriguez, J. *J. Phys. Chem.* **1994**, *98*, 12059.
(32) Rodriguez, J. A.; Hrbek, J. *J. Phys. Chem.* **1994**, *98*, 4061.
(33) (a) Twigg, M. V., Ed. *Catalyst Handbook*, 2nd ed.; Wolfe Med.: Harcourt Brace, 1995. (b) Somorjai, G. A. *Introduction to Surface Chemistry and Catalysis*; Wiley: New York, 1994.
(34) Kittel, C. *Introduction to Solid State Physics*, 6th ed.; Wiley: New York, 1986; p 55.
(35) Wagner, C. D.; Gale, L. H.; Raymond, R. H. *Anal. Chem.* **1979**, *51*, 466.
(36) Schwaha, K.; Spencer, N. D.; Lambert, R. M. *Surf. Sci.* **1979**, *81*, 273.
(37) Lewis, J.; Schwarzenbach, D.; Flack, H. D. *Acta Crystallogr. A* **1982**, *38*, 733.
(38) (a) Abrahams, S. C.; Berstein, J. L. *Acta Crystallogr. B* **1969**, *25*, 1233. (b) Lehn, J. M.; Wipff, G.; Demuynck, J. *Chem. Phys. Lett.* **1980**, *76*, 344.
(39) (a) Slater, J. C. *Quantum Theory of Molecules and Solids*; McGraw-Hill: New York, 1965; Vol. 2, p 324. (b) Puschmann, A.; Haase, J. *Surf. Sci.* **1984**, *144*, 559.
(40) See pp 23 and 76 in ref 34 .
(41) Huber, K. P.; Herzberg, G. *Molecular Spectra and Molecular Structure IV: Constants of Diatomic Molecules*; Van Nostrand-Reinhold: New York, 1974.
(42) (a) Dance, I. G. *Inorg. Chem.* **1981**, *20*, 1487. (b) Wells, A. F. *Structural Inorganic Chemistry*, 5th ed.; Oxford University Press: New York, 1987.
(43) Ciraci, S.; Batra, I. P. *Phys. Rev. B* **1983**, *28*, 982.
(44) Michaelson, H. B. *J. Appl. Phys.* **1977**, *48*, 4729.
(45) Baer, Y.; Hedén, P. F.; Hedman, J.; Klasson, M.; Nordling, C.; Siegbahn, K. *Solid State Commun.* **1970**, *8*, 517.
(46) Causa, M.; Dovesi, R.; Pisani, C.; Roetti, C. *Surf. Sci.* **1989**, *215*, 259.
(47) (a) Koutecky, J.; Fantucci, F. *Chem. Rev.* **1986**, *86*, 539. (b) Hermann, K.; Bagus, P. S.; Nelin, C. J. *Phys. Rev. B* **1987**, *35*, 9467.
(48) Dyke, J. M.; Golob, L.; Jonathan, N.; Morris, A. *J. Chem. Soc., Faraday Trans. 2* **1975**, *71*, 1026.
(49) (a) Lide. D. R., Ed. *CRC Handbook of Chemical Physics*, 73rd ed.; CRC Press: Boca Raton, FL, 1992; p 9−129. (b) Smoes, S.; Mandy, F.; Vander Auwera-Mahieu, A.; Drowart, J. *Bull. Soc. Chim. Belg.* **1972**, *81*, 45.
(50) (a) Stohr, J.; Outka, D. A. *J. Vac. Sci. Technol. A* **1987**, *5*, 919. (b) Selmani, A.; Sichel, J. M.; Salahub, D. R. *Surf. Sci.* **1985**, *157*, 208. (c) Backx, C.; de Groot, C. P. M.; Biloen, P. *Surf. Sci.* **1981**, *104*, 300. (d) Van Santen, R. A.; Kuipers, H. P. C. E. *Adv. Catal.* **1987**, *35*, 265.
(51) (a) Mitchell, K. A. R. *Surf. Sci.* **1985**, *149*, 93. (b) Hayek, K.; Glassl, H.; Gutmann, A.; Leonhard, H.; Prutton, M.; Tear, S. P.; Welton-Cook, M. R. *Surf. Sci.* **1985**, *152/153*, 419. (c) Wong, P. C.; Zhou, M. Y.; Hui, K. C.; Mitchell, K. A. R. *Surf. Sci.* **1985**, *163*, 172.
(52) Rodriguez, J. A.; Kuhn, M.; Hrbek, *J. Chem. Phys. Lett.* **1996**, *251*, 13.
(53) (a) Hay, P. J.; Martin, R. L. *J. Chem. Phys.* **1985**, *83*, 5174. (b) Bauschlicher, C. W.; Nelin, C. J.; Bagus, P. S. *J. Chem. Phys.* **1985**, *82*, 3265.
(54) (a) Rodriguez, J. A. *Langmuir* **1991**, *7*, 1206. (b) Rodriguez, J. A. *Surf. Sci.* **1990**, *226*, 101. (c) Rodriguez, J. A. *Surf. Sci.* **1990**, *230*, 335. (d) Rodriguez, J. A. *Surf. Sci.* **1992**, *278*, 326.